

Uranyl Coordination in Ionic Liquids: The Competition between Ionic Liquid Anions, Uranyl Counterions, and Cl^- Anions Investigated by Extended X-ray Absorption Fine Structure and UV–Visible Spectroscopies and Molecular Dynamics Simulations

C. Gaillard,^{*,†} A. Chaumont,[‡] I. Billard,[†] C. Hennig,[§] A. Ouadi,[†] and G. Wipff^{*,‡}

Institut Pluridisciplinaire Hubert Curien, DRS, Chimie Nucléaire, 23 Rue du Lœss, 67037 Strasbourg Cedex 2, France, Laboratoire MSM, UMR 7177, Institut de Chimie, 4 Rue B. Pascal, 67000 Strasbourg, France, and Institute of Radiochemistry, Forschungszentrum Rossendorf, P.O. Box 510119, 01314 Dresden, Germany

Received September 28, 2006

The first coordination sphere of the uranyl cation in room-temperature ionic liquids (ILs) results from the competition between its initially bound counterions, the IL anions, and other anions (e.g., present as impurities or added to the solution). We present a joined spectroscopic (UV–visible and extended X-ray absorption fine structure)-simulation study of the coordination of uranyl initially introduced either as UO_2X_2 salts ($\text{X}^- = \text{nitrate } \text{NO}_3^-$, triflate TfO^- , perchlorate ClO_4^-) or as $\text{UO}_2(\text{SO}_4)$ in a series of imidazolium-based ILs (C_4mimA , $\text{A}^- = \text{PF}_6^-$, Tf_2N^- , BF_4^- and $\text{C}_4\text{mim} = 1\text{-methyl-3-butyl-imidazolium}$) as well as in the $\text{Me}_3\text{NBUtF}_2\text{N}$ IL. The solubility and dissociation of the uranyl salts are found to depend on the nature of X^- and A^- . The addition of Cl^- anions promotes the solubilization of the nitrate and triflate salts in the C_4mimPF_6 and the C_4mimBF_4 ILs via the formation of chloro complexes, also formed with other salts. The first coordination sphere of uranyl is further investigated by molecular dynamics (MD) simulations on associated versus dissociated forms of UO_2X_2 salts in C_4mimA ILs as a function of A^- and X^- anions. Furthermore, the comparison of $\text{UO}_2\text{Cl}_4^{2-}$, 2 X^- complexes with dissociated X^- anions, to the UO_2X_2 , 4 Cl^- complexes with dissociated chlorides, shows that the former is more stable. The case of fluoro complexes is also considered, as a possible result of fluorinated IL anion's degradation, showing that $\text{UO}_2\text{F}_4^{2-}$ should be most stable in solution. In all cases, uranyl is found to be solvated as formally anionic $\text{UO}_2\text{X}_n\text{A}_m\text{Cl}_p^{2-n-m-p}$ complexes, embedded in a cage of stabilizing IL imidazolium or ammonium cations.

Introduction

The management of highly radioactive waste represents a very important concern and is considered in terms of its ultimate disposal or its reprocessing by partitioning and further transmutation. Traditionally the removal of actinides by liquid–liquid extraction has focused on the use of organic solvents that can have high hazard ratings and low flash points resulting in health and safety concerns. In contrast to the traditional extracting phases, low melting organic salts known as ionic liquids (ILs) possess negligible flammability and volatility and therefore represent a new class of “green”

solvents that are inherently safer.^{1,2} ILs are composed of large organic cations like imidazolium, ammonium, or pyrrolidinium cation derivatives combined with various anions. They exhibit good radiochemical stability^{3,4} and, according to the combination of the anion and cation, their properties (viscosity, hydrophobicity, melting point, miscibility to water,

* To whom correspondence should be addressed. E-mail: cgaillard@ires.in2p3.fr (C.G.), wipff@chimie.u-strasbg.fr (G.W.).

† Institut Pluridisciplinaire Hubert Curien.

‡ Institut de Chimie.

§ Forschungszentrum Rossendorf.

(1) Welton, T. *Chem. Rev.* **1999**, *99*, 2071.

(2) Rogers, R. D.; Seddon, K. R. In *Ionic Liquids: Industrial Applications for Green Chemistry*; Rogers, R. D., Seddon, K. R., Eds.; ACS Symposium Series; American Chemical Society: Washington DC, 2002; p 818.

(3) Allen, D.; Baston, G. M.; Bradley, A. E.; Gorman, T.; Haile, A.; Hamblett, I.; Hatter, J. E.; Healey, M. J.; Hodgston, B.; Lewin, R.; Lovell, K. V.; Newton, B.; Pitner, W. R.; Rooney, D. W.; Sanders, D.; Seddon, K. R.; Sims, H. E.; Thied, R. C. *Green Chem.* **2002**, *4*, 152.

(4) Berthon, L.; Nikitenko, S.; Bisel, I.; Berthon, C.; Faucon, M.; Saucerotte, B.; Zorz, N.; Moisy, P. *Dalton Trans.* **2006**, 2526.

etc.) can be tailored,⁵ presenting great potentials for their use in the field of nuclear waste reprocessing. Also, some ILs present good ionic conductivity and a wide electrochemical window as compared to water or classical organic solvents,^{6,7} and thus electrolytic metal deposition of actinides^{8,9} in ILs may be envisioned. It has been shown that Th(IV) can be reduced to Th(0) in Me₃NBuTf₂N and that this reduction proceeds more easily in this IL than in other nonaqueous solvents.¹⁰ Several studies have also shown the possible use of ILs for liquid–liquid extraction in replacement of traditional solvents^{11–16} or by the use of task-specific ionic liquids, i.e., ILs on which the complexing moieties are grafted on the IL cationic part.^{17–19} Whereas cationic species are extracted into conventional organic solvents as neutral complexes, in an IL phase they can be extracted either as cationic or as neutral species, depending on the hydrophobicity of the chosen IL components.^{20,21} For instance, the mechanism of extraction of uranium(VI) and trivalent actinides/lanthanides (Eu³⁺, Am³⁺) by dialkylphosphoric acid is identical (i.e., by extraction of neutral complexes) in dodecane and in the very hydrophobic IL C₁₀mimTf₂N.²² On the other hand, Am³⁺, UO₂²⁺, Pu⁴⁺, and Th⁴⁺ are extracted by CMPO/TBP to a less hydrophobic IL, C₄mimPF₆, through a cation exchange mechanism.²³ More fundamental studies have also evidenced the influence of ILs on the chemical properties of An/Ln. For example, AnCl₆²⁻ (An = Np, Pu)

species, which are sensitive to hydrolysis, are stable in ILs even in the presence of a large amount of water.^{24,25} Those studies show that the unusual nature of ionic liquids leads to complex phenomena which understanding requires fundamental knowledge of the chemistry and reactivity of species like lanthanides and actinides. So far, coordination properties of IL entities are mostly studied in the solid state,^{26,27} and investigations in the liquid state are rare.^{28,29} We thus decided to extend our studies on the solvation of trivalent europium in a series of ILs³⁰ to the case of U(VI).

The aim of this work is to gain insight into the coordination properties of uranyl in ILs, as a function of the nature of the uranyl counterions and of the ionic liquid. Using UV–visible spectroscopy and extended X-ray absorption fine structure (EXAFS), we investigate the coordination sphere of uranyl after dissolution of various uranyl salts (UO₂X₂ with X⁻ = NO₃⁻, triflate TfO⁻, ClO₄⁻ and UO₂SO₄) in four different ionic liquids. Three of them (C₄mimPF₆, C₄mimTf₂N, and C₄mimBF₄) are based on the imidazolium cation (C₄mim = 1-methyl-3-butyl-imidazolium) and differ by their anionic components (PF₆⁻, (CF₃SO₂)₂N⁻ hereafter noted as Tf₂N⁻, and BF₄⁻, respectively), while the Me₃NBuTf₂N liquid is based on a quaternary ammonium Me₃NBu⁺ cation, allowing us to assess the role of anionic and cationic components of the liquid. As a reference for fully dissociated UO₂X₂ salts in the C₄mimTf₂N liquid, we also report the UV–visible spectrum of the UO₂(Tf₂N)₂ salt dissolved in that liquid, where the uranyl cation thus should coordinate to the Tf₂N⁻ anions only. We further investigate the reactivity of the uranyl toward chloride ions introduced in solutions. These studies are complemented by molecular dynamics (MD) simulations on selected systems, providing microscopic insights into the solvation of uranyl salts in their associated versus dissociated forms. The effect of added competitive Cl⁻ anions is also simulated in three liquids with selected uranyl salts.

Methods

1. Experimental. The ILs C₄mimTf₂N, C₄mimPF₆, C₄mimBF₄, Me₃NBuTf₂N (purity ≥99%), and C₄mimCl (purity 98%) were purchased from Solvionic. Uranyl salts were either synthesized in our laboratory,³¹ uranyl triflate (UO₂(CF₃SO₃)₂), uranyl perchlorate (UO₂(ClO₄)₂), and (UO₂(Tf₂N)₂), or purchased, uranyl nitrate (UO₂(NO₃)₂·6H₂O from Fluka) and uranyl sulfate (UO₂SO₄·2H₂O from Prolabo).

The same uranyl samples were analyzed by EXAFS and UV–visible spectroscopy. After dissolution of the salts in the ionic liquid, samples were degassed under vacuum at 60 °C for 10 h. After

- (5) Huddleston, J. G.; Visser, A. E.; Reichert, W. M.; Willauer, H. D.; Broker, G. A.; Rogers, R. D. *Green Chem.* **2001**, *3*, 156.
 (6) Suarez, P. A.; Einloft, S.; Dullius, J. E.; De Souza, R. F.; Dupont, J. J. *Chem. Phys.* **1998**, *95*, 1626.
 (7) Oldham, W. J.; Costa, D. A.; Smith, W. H. In *Ionic Liquids: Industrial Applications for Green Chemistry*; Rogers, R. D., Seddon, K. R., Eds.; ACS Symposium Series; American Chemical Society: Washington, DC, 2002; Vol. 15, p 188.
 (8) Bhatt, A. I.; May, I.; Volkovich, V. A.; Collison, D.; Helliwell, M.; Polovov, I. B.; Lewin, R. *Inorg. Chem.* **2005**, *44*, 4934.
 (9) Baston, G. M.; Bradley, A. E. Ionic Liquids for the Nuclear Industry: A Radiochemical, Structural and Electrochemical Investigation. In *Ionic Liquids: Industrial Applications for Green Chemistry*; Rogers, R. D., Seddon, K. R., Eds.; ACS Symposium Series; American Chemical Society: Washington DC, 2002; p 162.
 (10) Bhatt, A. I.; Duffy, N. W.; Collison, D.; May, I.; Lewin, R. G. *Inorg. Chem.* **2006**, *45*, 1677.
 (11) Gaillard, C.; Moutiers, G.; Mariet, C.; Antoun, T.; Gadenne, B.; Hesemann, P.; Moreau, J. J. E.; Ouadi, A.; Labet, A.; Billard, I. In *Ionic Liquids III: Fundamentals, Progress, Challenges, and Opportunities*; Rogers, R. D., Seddon, K. R., Eds.; Oxford University Press: New York, 2005; Vol. B, p 19.
 (12) Jensen, M. P.; Neufeind, J.; Beitz, J. V.; Skanthakumar, S.; Soderholm, L. *J. Am. Chem. Soc.* **2003**, *125* (50), 15466.
 (13) Guoxin, T.; Yongjun, Z.; Jingming, X.; Ping, Z. *Inorg. Chem.* **2003**, *42*, 735.
 (14) Dai, S.; Ju, Y. H.; Barnes, C. E. *J. Chem. Soc., Dalton Trans.* **1999**, 1201.
 (15) Jensen, M. P.; Dzielawa, J. A.; Rickert, P.; Dietz, M. L. *J. Am. Chem. Soc.* **2002**, *124*, 10664.
 (16) Visser, A. E.; Swatloski, R. P.; Reichert, W. M.; Griffin, S. T.; Rogers, R. D. *Ind. Eng. Chem. Res.* **2000**, *39*, 3596.
 (17) Visser, A. E.; Swatloski, R. P.; Reichert, W. M.; Mayton, R.; Sheff, S.; Wierzbicki, A.; Rogers, R. D. *Environ. Sci. Technol.* **2002**, *36*, 2523.
 (18) Ouadi, A.; Gadenne, B.; Hesemann, P.; Moreau, J. J. E.; Billard, I.; Gaillard, C.; Mekki, S.; Moutiers, G. *Chem.—Eur. J.* **2006**, *12*, 3074.
 (19) Lee, S.-G. *Chem. Commun.* **2006**, 1049.
 (20) Dietz, M. L.; Stepinski, D. C. *Green Chem.* **2005**, *7*, 747.
 (21) Dietz, M. L.; Dzielawa, J. A.; Laszak, I.; Young, B. A.; Jensen, M. P. *Green Chem.* **2003**, *5*, 682.
 (22) Cocalia, V. A.; Jensen, M. P.; Holbrey, J. D.; Spear, S. K.; Stepinski, D. C.; Rogers, R. D. *Dalton Trans.* **2005**, 1966.
 (23) Visser, A. E.; Rogers, R. D. *J. Solid State Chem.* **2003**, *171*, 109.

- (24) Nikitenko, S.; Moisy, P. *Inorg. Chem.* **2006**, *45*, 1235.
 (25) Schurhammer, R.; Wipff, G. *J. Phys. Chem. B* **2007**, *110*, 4659.
 (26) Mudring, A.-V.; Babai, A.; Arenz, S.; Giernoth, R. *Angew. Chem., Int. Ed.* **2005**, *44*, 5485.
 (27) Cocalia, V. A.; Gutowski, K. E.; Rogers, R. D. *Coord. Chem. Rev.* **2006**, *250*, 755.
 (28) Driesen, K.; Nockemann, P.; Binnemans, K. *Chem. Phys. Lett.* **2004**, *395*, 306.
 (29) Billard, I.; Mekki, S.; Gaillard, C.; Hesemann, P.; Moutiers, G.; Mariet, C.; Labet, A.; Bunzli, J. C. *Eur. J. Inorg. Chem.* **2004**, 1190.
 (30) Gaillard, C.; Billard, I.; Chaumont, A.; Mekki, S.; Ouadi, A.; Denecke, M. A.; Moutiers, G.; Wipff, G. *Inorg. Chem.* **2005**, *44*, 8355.
 (31) Bouby, M. Thesis, University L. Pasteur, Strasbourg, France, 1998.

Table 1. Summary of the Samples Analyzed by UV–Visible Spectroscopy and EXAFS^a

IL	composition	[Cl]/[U] ratio	sample acronym
C ₄ mimTf ₂ N	uranyl nitrate	0	Tf ₂ N_NO ₃
	uranyl nitrate + C ₄ mimCl	4	Tf ₂ N_NO ₃ _Cl
	uranyl perchlorate	0	Tf ₂ N_ClO ₄
	uranyl perchlorate + C ₄ mimCl	4	Tf ₂ N_ClO ₄ _Cl
	uranyl triflate	0	Tf ₂ N_TfO
	uranyl triflate + C ₄ mimCl	4	Tf ₂ N_TfO_Cl
C ₄ mimPF ₆	UO ₂ (Tf ₂ N) ₂	0	Tf ₂ N_Tf ₂ N ^b
	0.010 M uranyl nitrate + C ₄ mimCl	4	PF ₆ _NO ₃ _Cl
	0.010 M uranyl triflate + C ₄ mimCl	4	PF ₆ _TfO_Cl
C ₄ mimBF ₄	0.010 M uranyl nitrate + C ₄ mimCl	4	BF ₄ _NO ₃ _Cl
	0.010 M uranyl triflate + C ₄ mimCl	4	BF ₄ _TfO_Cl
Me ₃ NBuTf ₂ N	uranyl nitrate	0	Tf ₂ N _(Me₃NBu) _NO ₃
	uranyl nitrate + TBACl	4	Tf ₂ N _(Me₃NBu) _NO ₃ _Cl

^a Unless otherwise specified, the uranyl concentration is 0.02 M. ^b Analyzed only by UV–visible spectroscopy.

degassing, the solutions were immediately transferred and sealed in polyethylene containers in order to prevent any water reabsorption before their EXAFS analysis. Their residual water content, measured by the Karl Fischer titration after the XAS experiments, was found to be below 50 ppm (0.004 M, detection limit of the Karl Fischer titration). This corresponds to less than one water molecule per uranyl cation.

Only clear uranyl solutions, whose compositions are given in Table 1, were analyzed by EXAFS and UV–visible spectroscopy. Indeed, some problems were encountered by dissolving some of the salts in ILs. The dissolution of uranyl sulfate was found to be impossible in any ILs, even at very low concentration. The introduction of a very large excess of C₄mimCl did not improve its solubility, and in every case the uranyl sulfate powder remained in the solution. In C₄mimPF₆ and C₄mimBF₄, the dissolution of uranyl nitrate and uranyl triflate resulted in very cloudy solutions, while uranyl perchlorate powder could not dissolve at all. In the latter case, addition of a large excess of chloride ions in solution, as C₄mimCl, allowed only a slight dissolution of the salt. A summary of dissolution experiments is given in Supporting Information (Table S1 in Supporting Information).

UV–visible absorption spectra were recorded at room temperature on a Varian Cary 100 spectrophotometer between 16 700 and 33 300 cm⁻¹, using an empty cell as reference.

EXAFS experiments were carried out at ROBL-ESRF beamline, at the U L_{III} edge, in transmission mode using argon-filled ionization chambers at ambient temperature. The measurements were performed using a double crystal Si(111) monochromator. A yttrium foil was used for calibration in energy at 17 038 eV. EXAFS data reduction was made using the IFEFFIT code.³² Data analysis was carried out with the FEFFIT code,³³ using phase and back-scattering amplitude functions generated with the FEFF 8.1 code³⁴ from crystal structure data of Cs₂UO₂Cl₄, UO₂(NO₃)₂(H₂O)₂·H₂O, and UO₂(ClO₄)₂·3H₂O.^{35–37} Fits of the Fourier transform (FT) *k*³-weighted EXAFS data to the EXAFS equation were performed in *R*-space between 1 and 4 Å. The *k*-range used was 3.5–16 Å⁻¹. The amplitude reduction factor (*S*₀²) was held constant to 1 for all fits. The shift in the threshold energy (*E*₀) was allowed to vary as a global parameter for all atoms. In all fits, the coordination number of the uranyl oxygen atoms (*O*_{ax}) was held constant at 2. The 2-fold

degenerated four-legged multiple scattering path U–O_{ax1}–U–O_{ax2} was included in the curve fit by constraining its Debye–Waller factor and its effective path length to twice the values of the U–O_{ax} single-scattering path.

2. Molecular Dynamics. The different systems were simulated by classical molecular dynamics using the AMBER 7.0 software³⁸ in which the potential energy *U* is described by a sum of bond, angle, and dihedral deformation energy and a pairwise additive 1-6-12 (electrostatic and van der Waals) interaction between nonbonded atoms:

$$U = \sum_{\text{bonds}} k_b(r - r_0)^2 + \sum_{\text{angles}} k_\theta(\theta - \theta_0)^2 + \sum_{\text{dihedrals}} \sum_n V_n(1 + \cos(n\varphi - \gamma)) + \sum_{i < j} \left[\frac{q_i q_j}{R_{ij}} - 2\epsilon_{ij} \left(\frac{R_{ij}^*}{R_{ij}} \right)^6 + \epsilon_{ij} \left(\frac{R_{ij}^*}{R_{ij}} \right)^{12} \right] \quad (1)$$

Cross terms in van der Waals interactions were constructed using the Lorentz–Berthelot rules. Force field parameters for the pure ionic liquid were taken from the work of Andrade et al.³⁹ for the C₄mim⁺ and BF₄⁻ ions, while those for the PF₆⁻ anions were taken from the OPLS force field⁴⁰ and those of Tf₂N⁻ are from Canongia-Lopez and Pádua.⁴¹ These parameters have been shown to give good agreement with experimental data for the neat liquids.

The parameters of the UO₂²⁺ cation are those of Guilbaud and Wipff,⁴² while those for NO₃⁻, TfO⁻, and ClO₄⁻ are taken from the Baaden et al. work on lanthanide complexes.⁴³ The charges of SO₄²⁻ were fitted on ESP electrostatic potentials obtained at the HF/cc-pVTZ level. A summary of the atom types and charges is given in Figure S1. The 1-4 van der Waals interactions were scaled down by 2.0 and the 1-4 Coulombic interactions were scaled down by 1.2, as recommended by Cornell et al.⁴⁴ The pure liquids and solutions were simulated with 3D-periodic boundary conditions.

(32) Neville, M. *J. Synchrotron Radiat.* **2001**, *8*, 322.

(33) Neville, M.; Ravel, B.; Haskel, D.; Rehr, J. J.; Stern, A.; Yacoby, Y. *Physica B* **1995**, *208–209*, 154.

(34) Ankudinov, A.; Rehr, J. *J. Phys. Rev. B* **2000**, *62*, (4), 2437.

(35) Watkin, D. J.; Denning, R. G.; Prout, K. *Acta Crystallogr., Sect. C* **1991**, *47*, 2517.

(36) Shuvalov, R. R.; Burns, P. C. *Acta Crystallogr., Sect. C* **2003**, *59*, 71.

(37) Fischer, A. *Z. Anorg. Allg. Chem.* **2003**, *629*, 1012.

(38) Case, D. A.; Pearlman, D. A.; Caldwell, J. W.; Cheatham, T. E., III; Wang, J.; Ross, W. S.; Simmerling, C. L.; Darden, T. A.; Merz, K. M.; Stanton, R. V.; Cheng, A. L.; Vincent, J. J.; Crowley, M.; Tsui, V.; Gohlke, H.; Radmer, R. J.; Duan, Y.; Pitera, J.; Massova, I.; Seibel, G. L.; Singh, U. C.; Weiner, P. K.; Kollman, P. A. *AMBER7*; University of California: San Francisco, CA, 2002.

(39) de Andrade, J.; Böes, E. S.; Stassen, H. *J. Phys. Chem. B* **2002**, *106*, 3546.

(40) Kaminski, G. A.; Jorgensen, W. L. *J. Chem. Soc., Perkin Trans. 2* **1999**, *2*, 2365.

(41) Canongia-Lopes, J. N.; Padua, A. A. H. *J. Phys. Chem. B* **2004**, *108*, 16893.

(42) Guilbaud, P.; Wipff, G. *J. Mol. Struct.: THEOCHEM* **1996**, *366*, 55.

(43) Baaden, M.; Bery, F.; Madic, C.; Wipff, G. *J. Phys. Chem. A* **2000**, *104*, 7659.

Nonbonded interactions were calculated using a 12 Å atom based cutoff, correcting the long-range electrostatics by using the Ewald summation method in the particle mesh Ewald (PME) approximation.⁴⁵

The MD simulations were performed at 400 K in order to enhance the sampling, starting with random velocities, using the Verlet leapfrog algorithm with a time step of 2 fs to integrate the equations of motion. The temperature was monitored by coupling the system to a thermal bath using the Berendsen algorithm⁴⁶ with a relaxation time of 0.2 ps. All C–H bonds were constrained using the Shake algorithm.

We first equilibrated “cubic” boxes of pure liquids of about 40 Å length, containing about 200 pairs of C₄mim⁺A[−] ions (A[−] = Tf₂N[−], PF₆[−], or BF₄[−]). The resulting solvent densities (in g/cm³: 1.49 for C₄mimTf₂N, 1.33 for C₄mimPF₆, and 1.18 for C₄mimBF₄) were in reasonable agreement with experimental data (1.45, 1.36, and 1.20 g/cm³, respectively).⁴⁷ We then immersed the different uranyl salts (UO₂(TfO)₂, UO₂(NO₃)₂, UO₂(ClO₄)₂, or UO₂SO₄) under their dissociated (UO₂²⁺ + 2X[−], UO₂²⁺ + SO₄^{2−}) or associated (UO₂X₂, UO₂SO₄) form in the box. For the nitrate complex, we also considered the UO₂(NO₃)₂, NO₃[−] state with one dissociated nitrate and the complexed UO₂(NO₃)₃[−] state. The characteristics of the simulated systems are summarized in Table S2. Equilibration started with 1500 steps of steepest descend energy minimization, followed by 50 ps with fixed solutes (“BELLY” option in AMBER) at constant volume, and 50 ps of constant volume without constraints, followed by 50 ps at a constant pressure of 1 atm coupling the system to a barostat⁴⁶ with a relaxation time of 0.2 ps. Then MD was run for 5 ns in the (NVT) ensemble.

The MD trajectories were saved every 1 ps and analyzed with the MDS and DRAW software. Typical snapshots were redrawn using the VMD software. The average structure of the solvent around the UO₂²⁺ was characterized by the radial distribution functions (RDFs) of the anions and cations during the last 0.2 ns. The average coordination number (CN) of the solvent anions (O and N atoms of Tf₂N[−] and F and P atoms of PF₆[−]) and cations (N_{butyl} atom of C₄mim⁺) and its standard deviation were calculated up to a cutoff distance of the first peak of the RDF for the anion and up to 10 Å for the cation for which the first peak is less well-defined. Insights into energy features were obtained by group component analysis, using a 17 Å cutoff distance and a reaction field correction for the electrostatics. The total potential energy of the system in solution was decomposed as $E_{\text{tot}} = E_{\text{solute}} + E_{\text{solv}} + E_{\text{ILIL}}$, where E_{solute} is the internal energy of the solute in solution, E_{solv} is the solute/solvent interaction energy (“solvation energy”), and E_{ILIL} corresponds to the solvent/solvent interactions.

Results

As mentioned in the method section of this Article, some uranyl salts either were fully insoluble in the ionic liquids or could be solubilized only after addition of other solutes (Cl[−] salts). This therefore restricts the presentation of the spectroscopic analysis to the samples that are defined in Table 1. These are labeled in short by the sequence of anions

A_X (where A is the anion of the ionic liquid and X is the anion of the uranyl salt, also referred to as the uranyl counterion) or A_XCl when chloride salts have been added. Unless otherwise specified, the A[−] anion comes from the C₄mim⁺ based liquid, whereas A_{Me₃NBu} comes from the ammonium based liquid.

Two experimental techniques were used to analyze the samples, UV–visible spectroscopy and EXAFS, which are both sensitive to the local environment around uranium and give different kinds of information, especially when dealing with mixtures of complexes in solution. UV–visible absorption depends on the molar absorption coefficient ϵ of the different species in solution, and those that do not absorb or have a weak absorbance will hardly be detected and may be hidden by less concentrated but more absorbent ones. On the other hand, EXAFS is sensitive to all atoms present in the uranyl coordination spheres, and gives, in the case of a mixture of complexes, an average of the corresponding coordination numbers.

In the following text, we first discuss spectroscopic results. This is followed by the MD simulation results in two solvents.

Dissolution of Uranyl Salts in RTILs. Figure 1 exhibits the UV–visible spectra of samples obtained by dissolution of uranyl nitrate, uranyl triflate, and uranyl perchlorate in C₄mimTf₂N and Me₃NBuTf₂N. The spectrum of the UO₂(Tf₂N)₂ salt dissolved in the C₄mimTf₂N liquid (Figure 1) corresponds to the case where uranyl is fully surrounded by Tf₂N[−] anions. It exhibits six bands at 21 050, 21 835, 22 780, 23 530, 24 330, and 25 190 cm^{−1}, respectively, and can be considered as the signature of UO₂X₂ salts that would be fully dissociated in that liquid. Clearly, the UV spectra of all studied uranyl salts differ from that signature, indicating that they are solubilized in the IL without being fully dissociated.

We now turn to the case of nitrate salts. Spectra of samples Tf₂N_{NO₃} and Tf₂N_{Me₃NBu}NO₃ exhibit four intense bands at 21 370, 22 075, 22 830, and 23 530 cm^{−1}. The same bands have been observed upon dissolution of uranyl nitrate in acetone and attributed to the presence of the UO₂(NO₃)₃[−] complex which would exhibit a larger molar absorption coefficient than the other nitrate complexes.⁴⁸ It has been indeed proposed that the trinitrato-complex forms upon disproportionation of two UO₂(NO₃)₂ entities into UO₂(NO₃)₃[−] and UO₂(NO₃)⁺ complexes, but there is so far no indication on the extent of that process. Assuming that disproportionation also occurs in the ionic liquid solution, we can attribute the observed bands to the contribution of UO₂(NO₃)₃[−] species, in equilibrium with UO₂(NO₃)⁺ and possibly UO₂(NO₃)₂ and UO₂²⁺.

When changing the IL cation from C₄mim⁺ to Me₃NBu⁺, the aforementioned four intense bands remain unaltered. Slight differences are observed above 24 000 cm^{−1}, which may result from the influence of the solvent on the molar absorption coefficients of the species and/or from slight

(44) Cornell, W. D.; Cieplak, P.; Bayly, C. I.; Gould, I. R.; Merz, K. M.; Ferguson, D. M.; Spellmeyer, D. C.; Fox, T.; Caldwell, J. W.; Kollman, P. A. *J. Am. Chem. Soc.* **1995**, *117*, 5179.

(45) Darden, T. A.; York, D. M.; Pedersen, L. G. *J. Chem. Phys.* **1993**, *98*, 10089.

(46) Berendsen, H. J. C.; Postma, J. P. M.; van Gunsteren, W. F.; DiNola, A. *J. Chem. Phys.* **1984**, *81*, 3684.

(47) Tokuda, H.; Hayamizu, K.; Ishii, K.; Susan, M. A. B. H.; Watanabe, M. *J. Phys. Chem. B* **2004**, *108*, 16593.

(48) Rabinowitch, E.; Belford, R. L. *Spectroscopy and Photochemistry of Uranyl Compounds*; Macmillan: New York, 1964.

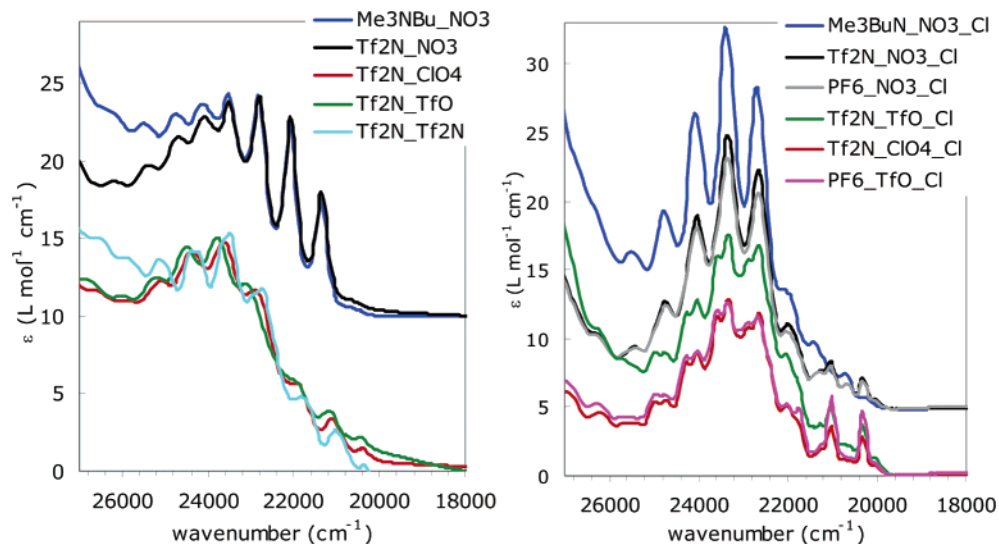


Figure 1. UV–visible spectra of uranyl solutions in ILs as a function of the dissolved salt (left) and in presence of chlorides (right). For the sake of clarity, A_NO₃ (left) and A_NO₃_Cl (right) spectra were shifted along the vertical axis.

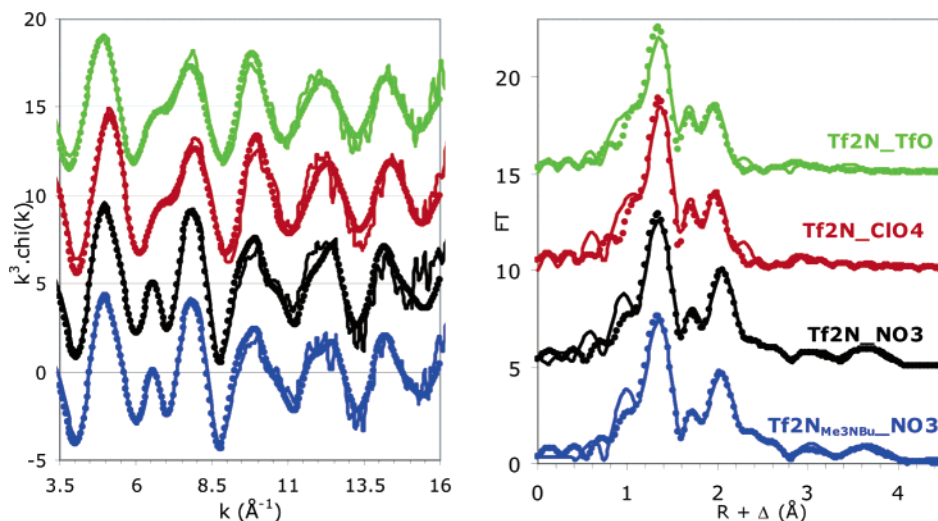


Figure 2. Influence of the uranyl salt and of IL on the solvation of uranium(VI): EXAFS spectra and their corresponding Fourier transform (uncorrected for phase shift Δ). For the sake of clarity, EXAFS and FT were shifted along the y-axis.

differences in uranyl speciation. These Tf₂N_NO₃ and Tf₂N_{Me₃NBu}_NO₃ spectra clearly indicate that the first coordination sphere of uranyl still comprises nitrate(s).

Tf₂N_CIO₄ and Tf₂N_TfO spectra clearly differ from the Tf₂N_NO₃ spectrum. They have the same shape as the Tf₂N_Tf₂N spectrum, but the positions of the six bands are slightly different for the three spectra. Taken together, these UV spectra indicate that the dissolution of uranyl nitrate, perchlorate, and triflate in BumimTf₂N does not involve a complete dissociation of those salts.

The samples were also analyzed by EXAFS, and the spectra are given in Figure 2, with the corresponding Fourier transforms. In all samples, FT signals are dominated by the large peak at $R + \Delta \sim 1.40$ Å, characteristic of the axial oxygen atoms of the uranyl group.

After dissolution of nitrate salts in C₄mimTf₂N and Me₃NBuTf₂N, their EXAFS spectra are identical. In particular, typical features arising from bidentate nitrate groups may be seen on the Fourier transforms, at $R + \Delta \sim 2.5$ Å and $R + \Delta \sim 3.6$ Å. The former arises from the nitrogen atoms,

and the latter feature is well reproduced by including in the fit the single path of the distal oxygen (O_d) and the multiple scattering paths (U–N–O_d) arising from the nitrate groups. Fitting results show the presence of approximately two nitrate groups in the coordination shell of uranyl, completed by approximately one additional oxygen atom. The average coordination of two nitrates per uranyl implies that all nitrates are coordinated to uranyl, which would be dissolved either in the form of the undissociated UO₂(NO₃)₂, UO₂(NO₃)₃[–] plus UO₂(NO₃)⁺ species, or their mixtures. Our EXAFS results are consistent with the presence of these different types of complexes but cannot alone afford the corresponding proportions. However, given the observed UV–visible spectroscopic signature of the [UO₂(NO₃)₃][–] species, one may conclude that a significant amount of the dissolved nitrate salt in the ionic liquid solution has disproportionated into equal amounts of [UO₂(NO₃)₃]⁺ and [UO₂(NO₃)₃][–] species.

After dissolution of perchlorate and triflate salts, their EXAFS spectra also look similar. The coordination sphere

of uranium is found to be composed of two axial oxygens at 1.75–1.76 Å and an average of four to five equatorial oxygen atoms at 2.42 Å. The same structural parameters were found for uranyl coordinated with Tf_2N^- anions in $\text{Me}_3\text{-NBuTf}_2\text{N}^{49}$ and are typical of an equatorial coordination of uranium(VI) to oxygen atoms, like in aqueous uranyl species.^{50,51} A priori, the oxygen atoms may stem from the uranyl counterions (ClO_4^- or TfO^-) as well as from Tf_2N^- solvent anions and/or water molecules.

To summarize, the combination of UV–visible and EXAFS measurements shows that the different salts of uranyl (nitrate, perchlorate, triflate), although well dissolved in $\text{C}_4\text{-mimTf}_2\text{N}$ and $\text{Me}_3\text{NBuTf}_2\text{N}$ ILs, remain, at least partially, associated.

Complexation to Chloride. The addition of chloride ions to the uranyl solutions entails a huge evolution of the UV–visible spectra, as a sign of the complexation between uranyl and Cl^- ions (see Figure 1). For samples $\text{PF}_6\text{-TfO-Cl}$, $\text{Tf}_2\text{N-TfO-Cl}$, and $\text{Tf}_2\text{N-ClO}_4\text{-Cl}$, the spectra are characteristic of the formation of the $\text{UO}_2\text{Cl}_4^{2-}$ complex.^{52–54} For samples $\text{Tf}_2\text{N}_{\text{Me}_3\text{NBu}}\text{-NO}_3\text{-Cl}$ and $\text{Tf}_2\text{N-NO}_3\text{-Cl}$, the bands maxima remain the same at 22 700, 23 420, 24 100, and 24 820 cm^{-1} but the fine structures are not observed anymore. These spectra can be compared to those obtained in acetone at different chlorides/uranyl ratios.⁵² In that case, addition of chlorides entails first a rise in the absorption, followed by a decrease when $\text{UO}_2\text{Cl}_4^{2-}$ is formed, indicating that the latter complex has the weakest absorption among all the chloro-species formed. As a result, the presence, even as minor species, of other complexes like UO_2Cl_2 or UO_2Cl_3^- may cause significant changes in the absorption spectrum. Thus, the shape of $\text{Tf}_2\text{N}_{\text{Me}_3\text{NBu}}\text{-NO}_3\text{-Cl}$ and $\text{Tf}_2\text{N-NO}_3\text{-Cl}$ spectra indicates that the complexation of chlorides to uranyl is not total at the studied 1:4 U/Cl ratio.

UV–visible spectra of samples $\text{BF}_4\text{-NO}_3\text{-Cl}$ and $\text{BF}_4\text{-TfO-Cl}$ are displayed in Figure 3. They exhibit a large background noise from which emerge weak peaks. The high background cannot be attributed to the ionic liquid absorption, since the C_4mimBF_4 does not absorb at those wavelengths.

Strong changes also occur in the EXAFS spectra when chlorides are introduced in solution (see Figure 4). In particular, FT of all those samples exhibit a peak at $R + \Delta \sim 2.25$ Å, which can be attributed to the presence of chloride ions in the uranyl coordination sphere. The intensity of this peak is very high for all samples, except for $\text{BF}_4\text{-TfO-Cl}$ and $\text{BF}_4\text{-NO}_3\text{-Cl}$. Fit results show that the $\text{UO}_2\text{Cl}_4^{2-}$ complex is formed in $\text{C}_4\text{mimTf}_2\text{N}$, $\text{Me}_3\text{NBuTf}_2\text{N}$, and C_4mimPF_6 . The

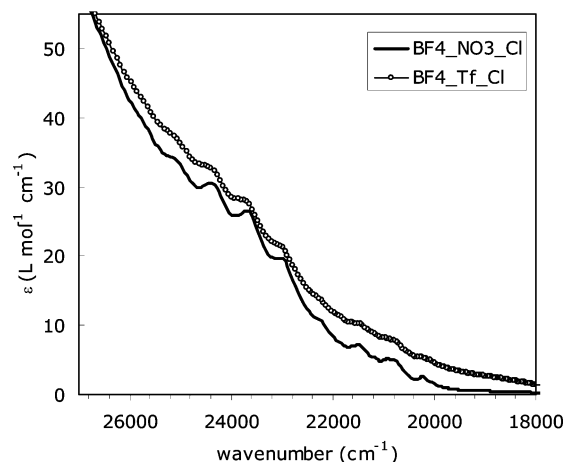


Figure 3. UV–visible spectra of uranyl nitrate and uranyl triflate in $\text{C}_4\text{-mimBF}_4$ in the presence of C_4mimCl .

structural parameters found for the tetrachloro-complex are similar to those obtained for the same species in acetonitrile,⁵³ with four U–Cl distances of ~ 2.69 Å. As observed in refs 50 and 53, the feature at $R + \Delta \sim 1.80$ Å on the Fourier transform could not be attributed to equatorial oxygens and is well reproduced by the fit with the chloride shell (see Figure S2). The small feature at $R + \Delta \sim 3.22$ Å on the Fourier transform could be well reproduced by including in the fit the multiple scattering path $\text{U-Cl-O}_{\text{ax}}\text{-U}$. Those results are fully consistent with UV–visible spectroscopy results for triflate and perchlorate samples. For nitrate based-samples ($\text{Tf}_2\text{N}_{\text{Me}_3\text{NBu}}\text{-NO}_3\text{-Cl}$, $\text{Tf}_2\text{N-NO}_3\text{-Cl}$, and $\text{PF}_6\text{-NO}_3\text{-Cl}$), UV–visible results suggest that the complexation is not total, while EXAFS gives an average coordination sphere of four chlorides, indicating that $\text{UO}_2\text{Cl}_4^{2-}$ is the major species. The presence of other species like UO_2Cl_3^- or UO_2Cl^+ cannot be precluded, but their proportion should be small, though. Thus, the chloride complexation is almost total.

In C_4mimBF_4 , the EXAFS spectra of samples $\text{BF}_4\text{-TfO-Cl}$ and $\text{BF}_4\text{-NO}_3\text{-Cl}$ are identical, which indicates a similar average coordination for uranyl in the two samples. Thus, the uranyl salts introduced in those solutions are likely dissociated. The intensity of the peak at $R + \Delta \sim 2.3$ Å on the FT, attributed to a chlorine shell, is weaker than the one of other spectra, indicating that the complexation of chlorides is only partial. The peak at $R + \Delta \sim 3.8$ Å, present in both spectra, cannot be explained by multiple scatterings occurring from nitrate groups since the sample $\text{BF}_4\text{-TfO-Cl}$ does not contain any nitrate ions. Thus, the uranyl salts introduced in those solutions are likely dissociated, which corroborates the fact that identical spectra were obtained for both samples. In this hypothesis (partial complexation to chlorides and dissociation of uranyl salts) and considering the species present in solution, one concludes that the equatorial shell of uranyl should be composed of chlorine and fluorine atoms. Moreover, the distance of the peak at ~ 3.8 Å on the FT is typical of U–U interactions via bridging ligands. The two spectra were thus fitted assuming a three shells model composed of fluorine, chlorine, and uranium. Because of the strong correlation between CN and σ^2 , we linked CN_{F} to CN_{Cl} to obtain a total equatorial CN equal to 5. Fit results

(49) Bhatt, A. I.; Kinoshita, H.; Koster, A. L.; May, I.; Sharrad, C.; Steele, H. M.; Volkovich, V. A.; Fox, O. D.; Jones, C. J.; Lewin, B. G.; Charnok, J. M.; Hennig, C. Proceedings of Atalante, Nimes, France, June 21–24, 2004.

(50) Allen, P. G.; Bucher, J. J.; Shuh, D. K.; Edelstein, N. M.; Reich, T. *Inorg. Chem.* **1997**, *36*, 4676.

(51) Gaillard, C.; El Azzi, A.; Billard, I.; Bolvin, H.; Hennig, C. *Inorg. Chem.* **2005**, *44*, 852.

(52) Görrler-Wallrand, C.; De Houwer, S.; Fluyt, L.; Binnemans, K. *Phys. Chem. Chem. Phys.* **2004**, *6*, 3292.

(53) Servaes, K.; Hennig, C.; Van Deun, R.; Görrler-Wallrand, C. *Inorg. Chem.* **2005**, *44*, 7705.

(54) Sornein, M.-O.; Cannes, C.; Le Naour, C.; Lagarde, G.; Simoni, E.; Berthet, J.-C. *Inorg. Chem.* **2006**, *45*, 10419.

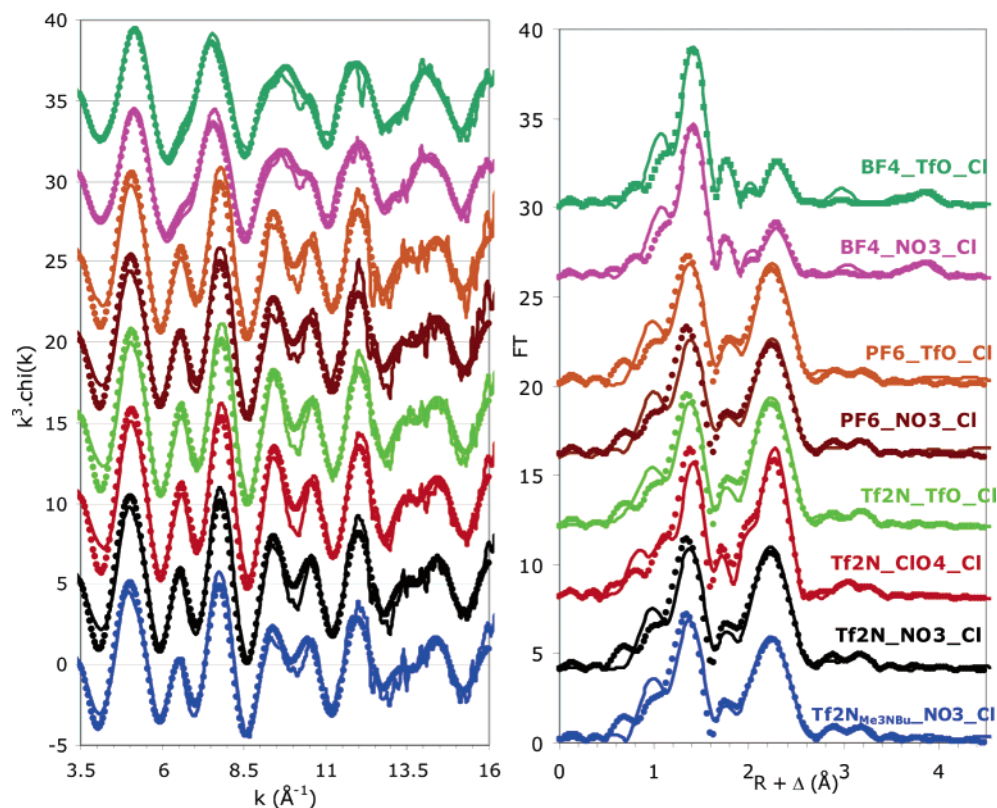


Figure 4. Influence of the uranyl salt and of IL on the complexation of uranium(VI) with chlorides: EXAFS spectra and their corresponding Fourier transform (uncorrected for phase shift Δ). For the sake of clarity, EXAFS and FT were shifted along the y-axis.

are displayed in Table 2. They show that the spectra can be well fitted by the chosen structural model. The average number of Cl atoms coordinated to an U atom is found to be ~ 1 . The U–Cl distance of 2.70–2.71 Å corresponds to a 5-fold equatorial coordination, as was observed for aquo–chloro complexes of uranyl, whereas a 4-fold coordination shows a shorter distance of 2.68 Å.⁵⁵ The coordination sphere of uranyl is completed by approximately four F atoms at 2.26–2.27 Å. It must be noticed that the Debye–Waller factor of the fluorine shell is quite large (0.016–0.017 Å²), which may indicate a wide disparity of bond lengths. The feature observed on both spectra at $R + \Delta \sim 3.8$ Å is well reproduced by a shell of approximately 1 U atom at 3.97 Å. This U–U distance is comparable to those observed in crystal structures of dimeric or polymeric uranyl complexes with bridging μ -F₂ ligands, where U–U distances are in the range 3.90–4.00 Å.^{56–60} In those compounds, U–F bond distances are in the range 2.30–2.39 Å,^{56–58} longer than those measured in monomeric uranyl complexes with fluoride and BF₄ anions in water (2.24 Å).^{51,61} Thus, the

intermediate U–F distance reported in our work (2.26–2.27 Å) would be consistent with the presence of dimeric or oligomeric fluoro-species, implying that fluoride ions are present in our samples. The degradation of fluorinated-based ILs to generate F[–] anions is a known process and has been, in particular, reported in the case of BF₄[–] in the presence of uranyl cations.⁵⁶ The partial complexation of chloride ions in C₄mimBF₄ (which contrasts with the total complexation observed in other ILs) may also be explained by the presence of competitive stronger ligands like fluoride.

As a conclusion, apart from C₄mimBF₄, we observed a quasi-complete complexation between uranyl and chloride ions in the studied ILs. As observed previously with europium(III),³⁰ uranyl has a strong affinity for chloride anions in the ILs, which contrasts to its low affinity in aqueous solutions.

Molecular Dynamics Results. Associated vs Dissociated UO₂(NO₃)₂, UO₂(TfO)₂, UO₂(ClO₄)₂, and UO₂SO₄ Salts in C₄mimPF₆ and C₄mimTf₂N Ionic Liquids. In this section, we describe the uranyl solvation in the C₄mimPF₆ and C₄mimTf₂N liquids, considering two important hypothetical states, namely, when the ions are dissociated (UO₂²⁺, 2X[–]; UO₂²⁺, SO₄^{2–}) and when they are associated (UO₂X₂ and UO₂SO₄). In principle, if the simulated time would be “infinite”, the simulations starting with either state should converge to a same situation, possibly leading, in some cases, to partial dissociation. This is not the case, however, as at the simulated time scale (5 ns), the salts retained their initial state, i.e., the dissociated salts remained

(55) Hennig, C.; Tutschku, J.; Rossberg, A.; Bernhard, G.; Scheinost, A. *C. Inorg. Chem.* **2005**, *44*, 6655.

(56) John, G. H.; May, I.; Collison, D.; Helliwell, M. *Polyhedron* **2004**, *23*, 3097.

(57) Walker, S. M.; Halasyamani, P. S.; Allen, S.; O’Hare, D. *J. Am. Chem. Soc.* **1999**, *121*, 10513.

(58) Almond, P. M.; Talley, C. E.; Bean, A. C.; Peper, S. M.; Albrecht-Schmitt, T. E. *J. Solid State Chem.* **2000**, *154*, 635.

(59) Cahill, C. L.; Burns, P. C. *Inorg. Chem.* **2001**, *40*, 1347.

(60) Allen, S.; Barlow, S.; Halasyamani, P. S.; Mosselmans, J. F.; O’Hare, D.; Walker, S. M.; Walton, R. I. *Inorg. Chem.* **2000**, *39*, 3791.

(61) Vallet, V.; Wahlgren, U.; Schimmelpennig, B.; Moll, H.; Szabo, Z.; Grenthe, I. *Inorg. Chem.* **2001**, *40*, 3516.

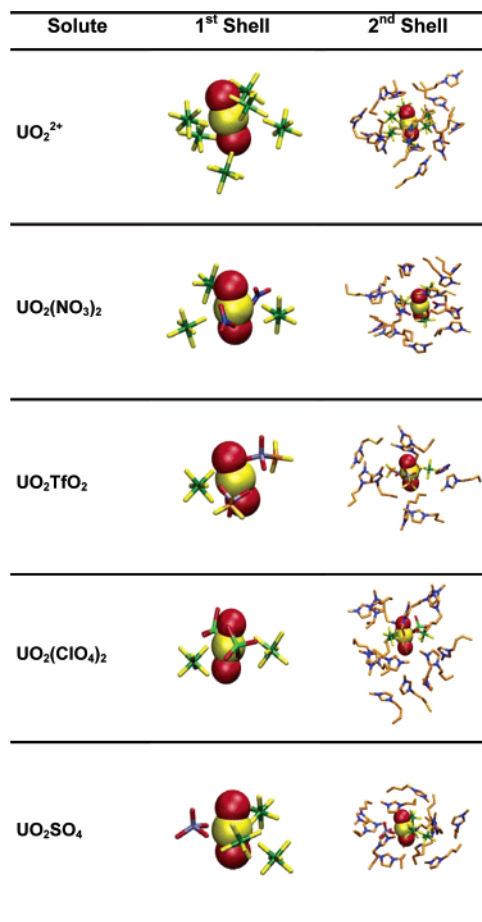
Table 2. Summary of the EXAFS Fit Results

sample	shell	CN ^a	R ^a	σ^2 ^a	
Tf ₂ N _{Me3NBu} _NO ₃	U–O _{ax}	2 ^b	1.76	0.002	$R_{\text{factor}} = 0.03$ $E_0 = -0.8$
	U–O _{eq}	1.0	2.42	0.002	
	U–O _N	3.8	2.51	0.006	
	U–N	1.9 ^c	2.92	0.002	
	U–O _d	1.9 ^c	4.17	0.003	
Tf ₂ N _{Me3NBu} _NO ₃ _Cl	U–O _{ax}	2 ^b	1.77	0.002	$R_{\text{factor}} = 0.04$ $E_0 = 6.0$
	U–Cl	3.3	2.69	0.005 ^b	
Tf ₂ N_NO ₃	U–O _{ax}	2 ^b	1.76	0.002	$R_{\text{factor}} = 0.02$ $E_0 = -0.9$
	U–O _{eq}	1.1	2.47	0.004	
	U–O _N	4.0	2.50	0.008	
	U–N	2 ^c	2.92	0.003	
Tf ₂ N_NO ₃ _Cl	U–O _{ax}	2 ^b	1.77	0.002	$R_{\text{factor}} = 0.05$ $E_0 = 6.0$
	U–Cl	3.5	2.69	0.005 ^b	
	U–O _{ax}	2 ^b	1.75	0.002	
Tf ₂ N_ClO ₄	U–O _{ax}	2 ^b	1.75	0.002	$R_{\text{factor}} = 0.05$ $E_0 = -0.5$
	U–O _{eq}	4.5	2.42	0.008	
Tf ₂ N_ClO ₄ _Cl	U–O _{ax}	2 ^b	1.77	0.002	$R_{\text{factor}} = 0.03$ $E_0 = 7.5$
	U–Cl	3.8	2.69	0.005 ^b	
Tf ₂ N_TfO	U–O _{ax}	2 ^b	1.76	0.002	$R_{\text{factor}} = 0.05$ $E_0 = -7.4$
	U–O _{eq}	4.4	2.42	0.008	
Tf ₂ N_TfO_Cl	U–O _{ax}	2 ^b	1.77	0.002	$R_{\text{factor}} = 0.04$ $E_0 = 7.6$
	U–Cl	3.7	2.69	0.005 ^b	
PF ₆ _NO ₃ _Cl	U–O _{ax}	2 ^b	1.78	0.002	$R_{\text{factor}} = 0.07$ $E_0 = 7.2$
	U–Cl	3.4	2.70	0.005 ^b	
PF ₆ _TfO_Cl	U–O _{ax}	2 ^b	1.78	0.002	$R_{\text{factor}} = 0.05$ $E_0 = 7.8$
	U–Cl	3.5	2.69	0.005 ^b	
BF ₄ _NO ₃ _Cl	U–O _{ax}	2 ^b	1.78	0.002	$R_{\text{factor}} = 0.05$ $E_0 = -1.8$
	U–F	3.5 ^d	2.26	0.016	
	U–Cl	1.5	2.70	0.005 ^b	
	U–U	0.8	3.97	0.006	
BF ₄ _TfO_Cl	U–O _{ax}	2 ^b	1.78	0.002	$R_{\text{factor}} = 0.05$ $E_0 = -1.4$
	U–F	3.8 ^d	2.27	0.017	
	U–Cl	1.2	2.71	0.005 ^b	
	U–U	1.0	3.97	0.007	

^a CN = coordination number $\pm 20\%$, R = distance ± 0.01 Å, σ^2 = Debye–Waller factor ± 0.002 Å². E_0 is the shift in threshold energy and R_{factor} is the goodness of the fit as defined in ref 33. ^b Held constant during the fit. ^c Held equal to half N_{Oeq}. ^d Linked to CN_{Cl}, assuming CN_F = 5 – CN_{Cl}.

so during all MD simulations, while the associated ones remained complexed, sometimes with different anion densities. The simulations cannot probe the solubility of the salts but provide microscopic insights into their solvation by the ILs, from structural and energetic points of view. Typical snapshots are presented in Figure 5 (C₄mimPF₆ solution) and Figure 6 (C₄mimTf₂N solution), and the characteristics of the RDFs are summarized in Tables 3 and 4. Tables 5 – 8 summarize the results of the energy analysis of the different systems in solution.

Dissociated Salts. In a given liquid, a similar solvent structure around the “naked” UO₂²⁺ cation is found for the different dissociated complexes. In C₄mimPF₆, its first solvation shell is formed by six monodentate PF₆[–] anions, three of them slightly beneath and three slightly above its equatorial plane (Figure 5), leading to a total coordination number of 6 for UO₂²⁺ (Table 3). In the C₄mimTf₂N liquid, UO₂²⁺ is surrounded by about five Tf₂N[–] anions that mainly coordinate monodentate via their oxygen atoms (Figure 6). However one or two Tf₂N[–] sometimes coordinate bidentate, leading to a CN of 6–7 (Table 4). In both liquids, the first solvation shell is surrounded by a positively charged second shell of 12 C₄mim⁺ cations in C₄mimPF₆ liquid and 10 C₄mim⁺ cations in C₄mimTf₂N.

**Figure 5.** Uranyl complexes in C₄mimPF₆: typical snapshots of the first and second solvation shell of UO₂²⁺.

UO₂(NO₃)₂ Associated Complexes. During the dynamics, in both liquids, the two NO₃[–] anions initially coordinated bidentate to uranyl turned monodentate. The resulting first shell of UO₂(NO₃)₂ is completed by three PF₆[–] monodentate anions, leading to a CN of 5 (2 O_{NO3} + 3 F_{PF6}). In order to assess the influence of the nitrate binding mode, we performed additional dynamics where the nitrates were constrained to remain bidentate. In that case, the number of PF₆[–] anions in the first solvation shell of uranyl is reduced to two, whereas the total CN increases to 6. All complexes are surrounded by a second solvation shell, of approximately 12 C₄mim⁺ cations up to 10 Å. In the C₄mimTf₂N solution, the first solvation shell of UO₂(NO₃)₂ comprises three monodentate Tf₂N[–] anions when the nitrates are monodentate and two monodentate Tf₂N[–] anions when the nitrates are constrained to be bidentate.

UO₂(TfO)₂ Associated Complexes. During the dynamics in the C₄mimPF₆ and C₄mimTf₂N liquids, both TfO[–] anions coordinate bidentate to the U atom at average U–O_{TfO} distances of about 2.6 Å. The first shell of the UO₂(TfO)₂ complex is completed by one bidentate PF₆[–] anion in C₄mimPF₆ and by two Tf₂N[–] anions (coordinated via one oxygen) in C₄mimTf₂N. In both liquids, the complex is surrounded by a second shell of 10–11 C₄mim⁺ cations in C₄mimPF₆ and 9 C₄mim⁺ cations in C₄mimTf₂N.

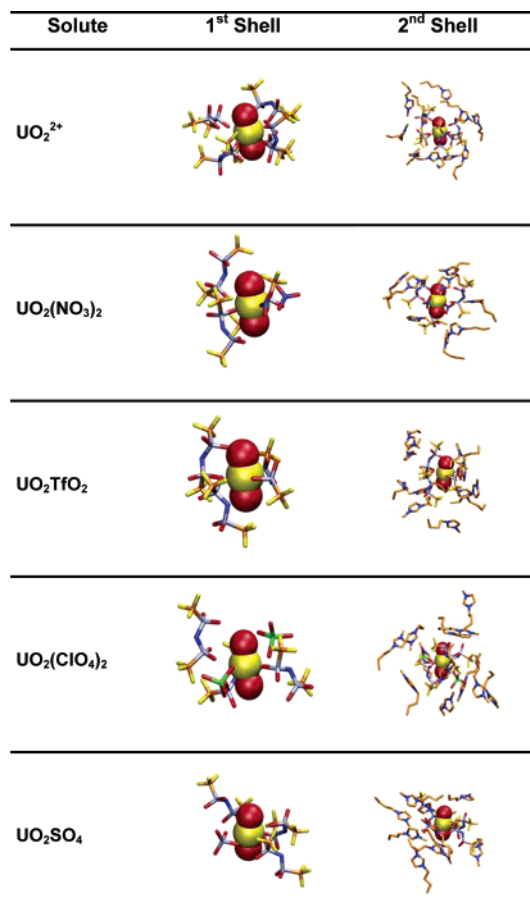


Figure 6. Uranyl complexes in C₄mimTf₂N: typical snapshots of the first and second solvation shell of UO₂²⁺.

Table 3. Main Characteristics of the Solvent RDFs around the U Atom in Uranyl Complexes in C₄mimPF₆

solute	F _{PF₆} ^a	P _{PF₆} ^a	N _{C₄mim} ^b
UO ₂ ²⁺ , 2NO ₃ ⁻	5.9 (2.55; 3.20)	5.4 (4.00; 4.80)	11.8
UO ₂ (NO ₃) ₂	3.0 (2.55; 3.15)	3.0 (4.05; 4.80)	12.5
UO ₂ (NO ₃) ₂ (ctr) ^c	2.1 (2.60; 3.20)	2.2 (4.10; 4.70)	12.9
UO ₂ ²⁺ , 2TfO ⁻	5.8 (2.50; 3.15)	5.7 (4.00; 5.10)	12.3
UO ₂ TfO ₂	2.0 (2.60; 3.30)	1.0 (3.60; 4.40)	10.3
UO ₂ ²⁺ , 2ClO ₄ ⁻	5.8 (2.55; 3.20)	5.0 (4.00; 4.80)	11.7
UO ₂ (ClO ₄) ₂	2.4 (2.50; 3.10)	2 (3.90; 4.45)	12.0
UO ₂ ²⁺ , SO ₄ ²⁻	5.8 (2.55; 3.20)	5.3 (4.00; 5.00)	12.9
UO ₂ SO ₄	3.1 (2.55; 3.05)	3.0 (4.00; 4.65)	11.7
UO ₂ ²⁺ , 5F ⁻	5.5 (2.55; 3.10)	5.3 (4.00; 4.95)	10.2
UO ₂ F ⁺ , 4F ⁻	4.3 (2.55; 3.20)	3.6 (3.95; 4.65)	11.6
UO ₂ F ₂ , 3F ⁻	2.9 (2.60; 3.20)	2.2 (3.90; 4.85)	10.8
UO ₂ F ₃ ⁻ , 2F ⁻	1.2 (2.55; 3.10)	1.0 (3.90; 4.85)	9.8
UO ₂ F ₄ ²⁻ , 1F ⁻	^d	^d	10.3

^a The first number corresponds to the coordination number. The second number indicates the distance (in Å) of the first peak, and the third number is the upper distance used to integrate the RDF. ^b Integration up to 10 Å. ^c The nitrates are constrained to be bidentate. ^d No solvent PF₆⁻ anions are in the first shell of UO₂²⁺.

UO₂(ClO₄)₂ Complex. In both liquids, the two ClO₄⁻ anions coordinate monodentate to UO₂²⁺ at average O_{ClO₄}-U distances of about 2.5 Å. In C₄mimPF₆, the first shell of uranyl is completed with two monodentate PF₆⁻ anions, while in C₄mimTf₂N it is completed by three Tf₂N⁻ anions coordinated via one of their oxygen atoms. This first shell

Table 4. Main Characteristics of the Solvent RDFs around the U Atom in Uranyl Salts in C₄mimTf₂N

solute	O _{Tf₂N}	N _{Tf₂N}	N _{C₄mim} ^b
UO ₂ ²⁺ , 2NO ₃ ⁻	6.3 (2.60; 3.10)	5.0 (4.55; 6.65)	9.7
UO ₂ (NO ₃) ₂	3.2 (2.50; 3.25)	3.0 (4.65; 5.30)	9.3
UO ₂ (NO ₃) ₂ (ctr) ^c	2.3 (2.60; 3.15)	2.0 (4.70; 5.55)	8.4
UO ₂ ²⁺ , 2TfO ⁻	5.6 (2.55; 3.00)	5.0 (4.65; 6.40)	10.3
UO ₂ TfO ₂	2.0 (2.55; 3.00)	2.0 (4.70; 5.15)	8.9
UO ₂ ²⁺ , 2ClO ₄ ⁻	6.3 (2.6; 3.15)	5.0 (4.60; 6.10)	8.8
UO ₂ (ClO ₄) ₂	3.2 (2.55; 3.10)	3.0 (4.65; 5.65)	9.0
UO ₂ ²⁺ , SO ₄ ²⁻	6.9 (2.55; 3.20)	5.0 (4.65; 5.55)	10.8
UO ₂ SO ₄	3.2 (2.50; 3.00)	3.0 (4.70; 5.50)	10.9

^aThe first number corresponds to the coordination number. The second number indicates the distance (in Å) of the first peak, and the last number indicates the upper distance used to integrate the RDF. ^b Integration up to 10 Å. ^c The nitrates are constrained to be bidentate.

Table 5. Energy Component Analysis (in kcal/mol) of Uranyl Salts in C₄mimPF₆

solute	E _{solute} ^a	E _{ILIL} ^b	E _{solv} ^c	E _{tot} ^d
UO ₂ ²⁺ , 2NO ₃ ⁻	-52	-6241	-675	-6968
UO ₂ (NO ₃) ₂	-367	-6495	-156	-7018
UO ₂ (NO ₃) ₂ (ctr) ^e	-409	-6512	-106	-7027
UO ₂ ²⁺ , 2TfO ⁻	114	-6248	-654	-6788
UO ₂ TfO ₂	-231	-6455	-86	-6772
UO ₂ ²⁺ , 2ClO ₄ ⁻	-64	-6199	-773	-7036
UO ₂ (ClO ₄) ₂	-154	-6471	-441	-7066
UO ₂ ²⁺ , SO ₄ ²⁻	-71	-6171	-798	-7040
UO ₂ SO ₄	-442	-6420	-222	-7084
UO ₂ ²⁺ , 5F ⁻	-116	-9285	-1035	-10436
UO ₂ F ⁺ , 4F ⁻	-337	-9442	-693	-10472
UO ₂ F ₂ , 3F ⁻	-476	-9479	-527	-10482
UO ₂ F ₃ ⁻ , 2F ⁻	-587	-9610	-397	-10594
UO ₂ F ₄ ²⁻ , 1F ⁻	-610	-9575	-417	-10602

^a Energy of UO₂X₂. ^b Energy of the liquid. ^c Interaction energy of UO₂X₂ with the IL. ^d E_{tot} = E_{solute} + E_{ILIL} + E_{solv}. ^e The nitrates are constrained to be bidentate.

Table 6. Energy Component Analysis (in kcal/mol) of Uranyl Salts in C₄mimTf₂N

solute	E _{solute} ^a	E _{ILIL} ^b	E _{solv} ^c	E _{tot} ^d
UO ₂ ²⁺ , 2NO ₃ ⁻	-70	5835	-674	5091
UO ₂ (NO ₃) ₂	-396	5603	-142	5065
UO ₂ (NO ₃) ₂ (ctr) ^e	-346	5609	-218	5045
UO ₂ (NO ₃) ₃ ⁻	-472	5560	-147	4941
UO ₂ (NO ₃) ₂ , NO ₃ ⁻	-411	5606	-230	4965
UO ₂ ²⁺ , 2TfO ⁻	101	5778	-644	5235
UO ₂ TfO ₂	-214	5567	-141	5212
UO ₂ ²⁺ , 2ClO ₄ ⁻	-49	5803	-694	5060
UO ₂ (ClO ₄) ₂	-307	5582	-206	5069
UO ₂ ²⁺ , SO ₄ ²⁻	-71	5867	-873	4923
UO ₂ SO ₄	-442	5623	-241	4940

^a Energy of UO₂X₂. ^b Energy of the liquid. ^c Interaction energy of UO₂X₂ with the IL. ^d E_{tot} = E_{solute} + E_{ILIL} + E_{solv}. ^e The nitrates are constrained to be bidentate.

is embedded in a cage of 12 C₄mim⁺ cations in the C₄mimPF₆ solution and 9 C₄mim⁺ in the C₄mimTf₂N solution.

UO₂SO₄ Complex. The SO₄²⁻ ion coordinates bidentate to uranyl during the dynamics in both liquids, at average U-O_{SO₄} distances of 2.37 Å. The first shell of the complex is completed by three monodentate PF₆⁻ anions in C₄mimPF₆ and by three monodentate Tf₂N⁻ anions in C₄mimTf₂N. Up to 10 Å, one finds a second shell formed of 11–12 C₄mim⁺ cations.

Table 7. Energy Component Analysis (in kcal/mol) of $\text{UO}_2\text{Cl}_4^{2-}$, 2X^- vs UO_2X_2 , 4Cl^- in C_4mimPF_6 Solution

solute	E_{solute}^a	E_{ILIL}^b	E_{solv}^c	E_{tot}^d
$\text{UO}_2(\text{NO}_3)_2, 4\text{Cl}^-$ (ctr) ^e	-445	-5962	-770	-7177
$\text{UO}_2\text{Cl}_4^{2-}, 2\text{NO}_3^-$	-584	-6097	-523	-7204
$\text{UO}_2\text{TfO}_2, 4\text{Cl}^-$	-249	-6046	-626	-6921
$\text{UO}_2\text{Cl}_4^{2-}, 2\text{TfO}^-$	-370	-6041	-592	-7003
$\text{UO}_2(\text{ClO}_4)_2, 4\text{Cl}^-$	-341	-6075	-665	-7081
$\text{UO}_2\text{Cl}_4^{2-}, 2\text{ClO}_4^-$	-547	-6030	-570	-7147

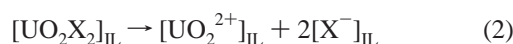
^a Energy of UO_2X_2 . ^b Energy of the liquid. ^c Interaction energy of UO_2X_2 with the IL. ^d $E_{\text{tot}} = E_{\text{solute}} + E_{\text{ILIL}} + E_{\text{solv}}$. ^e The nitrates are constrained to be bidentate.

Table 8. Energy Component Analysis (in kcal/mol) of $\text{UO}_2\text{Cl}_4^{2-}$, 2X^- vs UO_2X_2 , 4Cl^- in $\text{C}_4\text{mimTf}_2\text{N}$ Solution

solute	E_{solute}^a	E_{ILIL}^b	E_{solv}^c	E_{tot}^d
$\text{UO}_2(\text{NO}_3)_2, 4\text{Cl}^-$ (ctr) ^e	-424	5684	-638	4622
$\text{UO}_2\text{Cl}_4^{2-}, 2\text{NO}_3^-$	-52	5508	-848	4608
$\text{UO}_2\text{TfO}_2, 4\text{Cl}^-$	-219	5781	-688	4874
$\text{UO}_2\text{Cl}_4^{2-}, 2\text{TfO}^-$	-413	5722	-492	4817
$\text{UO}_2(\text{ClO}_4)_2, 4\text{Cl}^-$	-343	5739	-704	4692
$\text{UO}_2\text{Cl}_4^{2-}, 2\text{ClO}_4^-$	-559	5717	-471	4687

^a Energy of UO_2X_2 . ^b Energy of the liquid. ^c Interaction energy of UO_2X_2 with the IL. ^d $E_{\text{tot}} = E_{\text{solute}} + E_{\text{ILIL}} + E_{\text{solv}}$. ^e The nitrates are constrained to be bidentate.

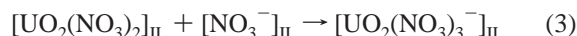
Energy Analysis of Dissociated Salts vs Associated Complexes. Since the simulations of the two forms of the salts have been performed with the same number of solvent and solute molecules, one can compare the corresponding total potential energies E_{tot} and gain insights into the preferred form, via eq 2. It should be noted that the fluctuations of



E_{tot} are quite large (approximately 50–60 kcal/mol), and hence small differences in E_{tot} should be interpreted with care. In the case of the $\text{UO}_2(\text{NO}_3)_2$ complex, the E_{tot} energy favors the associated form with bidentate ligands in both liquids, by approximately 45 kcal/mol in $\text{C}_4\text{mimTf}_2\text{N}$ and 60 kcal/mol in C_4mimPF_6 (Tables 5 and 6). For the other complexes, the results depend on the liquid. $\text{UO}_2(\text{TfO})_2$ prefers to be associated in $\text{C}_4\text{mimTf}_2\text{N}$ (by $\Delta E_{\text{tot}} \approx 20$ kcal/mol) and dissociated in C_4mimPF_6 solution ($\Delta E_{\text{tot}} \approx 15$ kcal/mol). For the $\text{UO}_2(\text{ClO}_4)_2$ complex, the dissociated salt is slightly privileged over the associated form in $\text{C}_4\text{mimTf}_2\text{N}$ (by approximately 10 kcal/mol), while the trend is reversed in C_4mimPF_6 where the associated form is favored (by approximately 30 kcal/mol). For the UO_2SO_4 complex, one sees that in C_4mimPF_6 the associated form is favored (by 45 kcal/mol) whereas in $\text{C}_4\text{mimTf}_2\text{N}$ the dissociated form is preferred (by 17 kcal/mol). Concerning the systems that have been studied by spectroscopy, we note the consensus concerning the state of nitrates that are complexed in the $\text{C}_4\text{mimTf}_2\text{N}$ solution. Triflates are also likely associated according to the MD simulations, which is also consistent with the fact that the UV spectrum obtained by dissolution of $\text{UO}_2(\text{TfO})_2$ differs from that of the dissolved $\text{UO}_2(\text{Tf}_2\text{N})_2$ salt. The weakly coordinating perchlorate somewhat prefers to be dissociated, thus following the decrease in uranyl–ligand interactions in the UO_2X_2 complex in the series where $\text{X} = \text{NO}_3^- > \text{TfO}^- > \text{ClO}_4^-$ (see Table S3).

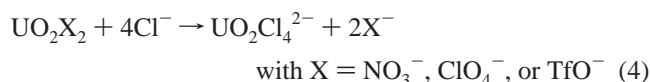
As the E_{tot} energy results from pairwise additive contributions of the solute, of the IL, and of their interactions ($E_{\text{tot}} = E_{\text{solute}} + E_{\text{ILIL}} + E_{\text{solv}}$), it is interesting to compare these components for the associated versus dissociated forms of the UO_2X_2 complexes (Tables 5 and 6). Upon dissociation, the E_{solute} energy markedly decreases, due to the reduced attractions between UO_2^{2+} and the two X^- anions, but this loss is compensated by a better solvation E_{solv} of the solute, also leading to less favorable interactions, E_{ILIL} , between the IL components.

As discussed in the case of nitrate complexes, other complexes, e.g., of UO_2X^+ or UO_2X_3^- types, might also be present in the studied solution. We thus decided to consider the following reaction that would correspond to the capture of one nitrate by $\text{UO}_2(\text{NO}_3)_2$ in the $\text{C}_4\text{mimTf}_2\text{N}$ IL:⁶²



In fact, the resulting change in E_{tot} is negative (–24 kcal/mol; Table 6), indicating that the trinitrate complex should be more stable in the IL solution in the case where nitrates are in excess, due to more favorable E_{solute} and E_{ILIL} energy components.

$\text{UO}_2\text{Cl}_4^{2-}$ vs $\text{UO}_2(\text{TfO})_2$, $\text{UO}_2(\text{ClO}_4)_2$, and $\text{UO}_2(\text{NO}_3)_2$ in Ionic Liquids. In order to study the effect of added Cl^- anions, we first considered the exchange reaction (eq 4) between the two coordinated X^- anions (NO_3^- , ClO_4^- , or TfO^-) and four Cl^- anions in both $\text{C}_4\text{mimTf}_2\text{N}$ and C_4mimPF_6 liquids.



As the initial and final states have been simulated with the same number of constituents, it is possible to compare their total potential energies E_{tot} . The results reported in Tables 7 and 8 show that with the three studied anions and in the two liquids, the final state is more stable, indicating that the Cl^- anions should displace the X^- anions initially coordinated to uranyl to form $\text{UO}_2\text{Cl}_4^{2-}$. In the $\text{C}_4\text{mimTf}_2\text{N}$ and C_4mimPF_6 liquids, the gain in E_{tot} amounts to approximately 15 and 30 kcal/mol, respectively, for the nitrate complex, 60 and 80 kcal/mol, respectively, for the triflate complex, and 5 and 60 kcal/mol for the perchlorate complex, respectively. These results are fully consistent with the experimental observation in the $\text{C}_4\text{mimTf}_2\text{N}$ and C_4mimPF_6 liquids where the salts could be dissolved (vide supra).

The competitive effect of Cl^- anions was similarly studied in the C_4mimBF_4 liquid, considering only the $\text{UO}_2(\text{TfO})_2$ salt which experimentally dissolves upon addition of a chloride salt.⁶³ The results given in Table 9 clearly indicate that the Cl^- anions should stepwise displace the triflate ligands from

(62) In principle, one could similarly model the disproportionation reaction of $\text{UO}_2(\text{NO}_3)_2$ in the IL but this would require using much bigger solvent boxes, leading to prohibitive computational costs.

(63) According to our MD simulations in the C_4mimBF_4 liquid, the equatorial shell of the UO_2TfO_2 complex comprises two bidentate TfO^- anions plus two BF_4^- anions, mostly monodentate, leading to a CN of 6.3 (4 O_{TfO} oxygens at 2.5 Å plus 2.3 F_{BF_4} atoms at 2.45 Å, on the average). The second shell contains 10.7 Bumim^+ cations, within 10 Å.

Table 9. Energy Component Analysis of Chloride Exchange around UO_2^{2+} in C_4mimBF_4

solute	E_{solute}^a	E_{LIL}^b	E_{sol}^c	E_{tot}^d
$\text{UO}_2\text{TfO}_2, 4\text{Cl}^-$	-219	-7364	-683	-8266
$\text{UO}_2\text{TfO}_2\text{Cl}_2^{2-}, 2\text{Cl}^-$	-371	-7450	-519	-8340
$\text{UO}_2\text{Cl}_2, 2\text{TfO}^- + 2\text{Cl}^-$	-274	-7413	-638	-8325
$\text{UO}_2\text{Cl}_4^{2-}, 2\text{TfO}^-$	-411	-7441	-513	8365

^a Energy of the solute. ^b Energy of the liquid. ^c Interaction energy between the solute and the liquid. ^d $E_{\text{tot}} = E_{\text{solute}} + E_{\text{LIL}} + E_{\text{sol}}$.

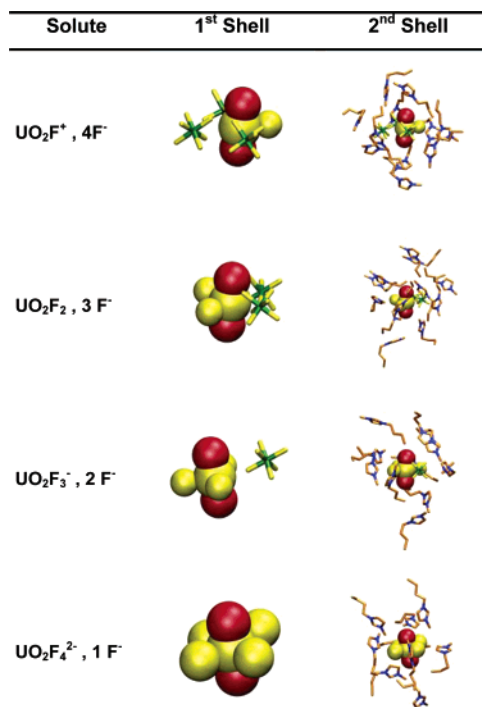
the complex, finally leading to the $\text{UO}_2\text{Cl}_4^{2-}$ species, which is favored by approximately 100 kcal/mol, compared to the $\text{UO}_2(\text{TfO})_2$ salt in the presence of remote Cl^- anions:



Thus, the lack of observation of the $\text{UO}_2\text{Cl}_4^{2-}$ complex in C_4mimBF_4 is not due to its instability in this liquid but to the formation of other complexes (uranyl dimers or oligomers) involving F ligands released from the BF_4^- degradation catalyzed by uranyl.

$\text{UO}_2\text{F}_n^{2-n}$ ($n = 1-5$) Complexes in the C_4mimPF_6 Ionic Liquid. The liquids based on F-containing anions like PF_6^- and BF_4^- may decompose and generate F^- anions that also compete with the other anions of the medium to solvate uranyl. This is why we decided to simulate the series of $\text{UO}_2\text{F}_n^{2-n}$ ($n = 1-5$) complexes in C_4mimPF_6 in order to compare their solvation and relative stabilities. Apart from the $\text{UO}_2\text{F}_5^{3-}$ complex that dissociates during dynamics to form $\text{UO}_2\text{F}_4^{2-}$, the other complexes remain stable during the whole dynamics. The resulting U–F equatorial distances with the F^- anions increase with the number of the latter, from 2.41 Å for UO_2F^+ to 2.46 Å for $\text{UO}_2\text{F}_4^{2-}$. Note that these distances are approximately 0.1 Å shorter than the U– F_{PF_6} ones (see Table 3). The first solvation shell of the unsaturated complexes is completed by a decreasing number of PF_6^- anions of the solvent: from 3.6 PF_6^- around UO_2F^+ to 1.0 PF_6^- around UO_2F_3^- and zero around $\text{UO}_2\text{F}_4^{2-}$ (Table 3 and Figure 7). The coordinated PF_6^- anions are mainly monodentate, leading to a total coordination number of 4–5 in the different fluoro complexes.

The comparison of the potential energy of the different systems (Table 5) reveals that the most stable one corresponds to the $\text{UO}_2\text{F}_4^{2-}$ complex that should therefore form in C_4mimPF_6 in the presence of F^- anions. The gain in total potential energy from the fully dissociated [$\text{UO}_2^{2+}, 5\text{F}^-$] to the tetrafluoro [$\text{UO}_2\text{F}_4^{2-}, \text{F}^-$] forms is quite high ($\Delta E_{\text{tot}} \approx 165$ kcal/mol) and results from antagonistic contributions. The coordination of four F^- anions to form $\text{UO}_2\text{F}_4^{2-}$ is intrinsically stabilizing for the solute itself ($\Delta E_{\text{solute}} \approx -500$ kcal/mol), but this is overcompensated by a loss in solvation energy ($\Delta E_{\text{sol}} \approx 600$ kcal/mol). The higher stability of the tetrafluoro complex thus mainly results from a more favorable intrasolvant energy ($\Delta E_{\text{LIL}} \approx 300$ kcal/mol). Combining this result with the lack of experimental evidence for the formation of the $\text{UO}_2\text{F}_4^{2-}$ complex in the C_4mimPF_6 solutions is indicative of negligible amounts of F^- anions in this solvent.

**Figure 7.** $\text{UO}_2\text{F}_n^{2-n}$ complexes in C_4mimPF_6 : typical snapshots of the first and second solvation shell of UO_2^{2+} .

Discussion

We report a joined spectroscopic and simulation study on the solvation of uranyl salts with different anions ($\text{X}^- = \text{NO}_3^-/\text{TfO}^-/\text{ClO}_4^-/\text{SO}_4^{2-}$) in a series of C_4mimA ionic liquids that differ by the anionic component ($\text{A}^- = \text{PF}_6^-/\text{Tf}_2\text{N}^-/\text{BF}_4^-$) and in the $\text{Me}_3\text{NBU}\text{Tf}_2\text{N}$ liquid based on an ammonium cation and Tf_2N^- . On the experimental side, insights into the solvation of uranyl are limited by the solubility of its salts in the ionic liquid and by the resolution of the resulting spectral data. Thus, spectroscopic data are available only in the $\text{C}_4\text{mimTf}_2\text{N}$ liquid for all UO_2X_2 salts and in C_4mimBF_4 and C_4mimPF_6 after addition of Cl^- ions that likely promote the dissolution of the salts. The UO_2SO_4 salt could not be solubilized and studied by spectroscopy. Molecular dynamics simulations, on the other hand, allow one to investigate selected hypothetical systems “in silico”, providing microscopic insights into structural and energy aspects of their solvation. Because of computer limitations, the MD studies were restricted to monomeric uranyl complexes in two liquids ($\text{C}_4\text{mimTf}_2\text{N}$ and C_4mimPF_6) and, as solutes, to the series of UO_2X_2 salts ($\text{X}^- = \text{NO}_3^-/\text{TfO}^-/\text{ClO}_4^-$) and UO_2SO_4 salts in their associated versus dissociated states. The possible formation of the UO_2X_3^- complex with nitrate anions was also explored in the $\text{C}_4\text{mimTf}_2\text{N}$ liquid. We also addressed computationally the question of Cl^- competition via a comparison of $\text{UO}_2\text{X}_2, 4\text{Cl}^-$ versus $\text{UO}_2\text{Cl}_4^{2-}, 2\text{X}^-$ in three liquids. Such computations are based on the hypothesis that the interactions in ionic liquid are mainly electrostatic + steric in nature, as generally assumed in MD studies on ionic liquids.⁶⁴ This does not mean that electronic reorganization effects (mainly charge transfer and

(64) Hunt, P. *Mol. Simul.* **2006**, *32*, 1.

polarization) are negligible, especially when hard species like UO_2^{2+} interact with soft (polarizable) species like the studied anions. However, the comparison with quantum mechanical results in the case of uranyl or europium complexes led to satisfactory agreement.^{65,30} Interactions between IL components are also satisfactorily depicted. In the case of the studied UO_2X_2 salts, the force field results also depict the main trends in binding energies, compared to HF/6-31G* or DFT(B3LYP)/6-31G* results (see Table S3).

Both spectroscopic and simulation studies support the view that the solvation of uranyl results from the competitive interactions between its initially coordinated counterions X^- , the anions A^- of the ionic liquid, plus possible added anions (like Cl^-). Uranyl in solution generally behaves as an $\text{UO}_2\text{X}_n\text{A}_m\text{Cl}_p^{2-n-m-p}$ anionic complex, with different equatorial atoms, depending on the salt(s) and the liquid. The complex is mainly stabilized in solution via its interactions with the positively charged surrounding shell of imidazolium or ammonium cations. Thus, the nature of the IL cationic component should not markedly determine the nature of the uranyl complex, as supported by the spectroscopic comparison of uranyl nitrate in the $\text{C}_4\text{mimTf}_2\text{N}$ and $\text{Me}_3\text{NBuTf}_2\text{N}$ liquids. Note however that a given $\text{UO}_2\text{X}_n\text{A}_m\text{Cl}_p^{2-n-m-p}$ complex should be better stabilized by imidazolium than by quaternary ammonium cations, which are more bulky and cannot afford H-bonding interactions with the anionic complex. This is consistent with spectroscopic results on $\text{UO}_2\text{Cl}_4^{2-}$ in different imidazolium based ILs⁶⁶ and by MD simulations on UCl_6^{2-} complexes in both ILs.²⁵

Among the studied anions, Cl^- interacts most strongly with uranyl, following the same trends as with the Eu^{3+} cation.³⁰ In the $\text{C}_4\text{mimTf}_2\text{N}$ and C_4mimPF_6 solutions of uranyl triflate or nitrate to which a chloride salt has been added, uranyl mainly exists in the form of the $\text{UO}_2\text{Cl}_4^{2-}$ anionic complex. In C_4mimBF_4 , experiments evidence a partial complexation which may be explained by the presence of fluoride anions formed by the decomposition of BF_4^- . As shown by MD and QM calculations,⁶⁷ fluorides are stronger ligands than chlorides and thus interfere in the complexation of uranyl with the latter. If uranyl–fluoro complexes were monomeric, the $\text{UO}_2\text{F}_4^{2-}$ species would be the most stable one, according to the simulations. In C_4mimBF_4 solution, however, the situation is more complex, likely involving dimeric and/or polymeric uranyl complexes, whose exact speciation would require more experiments.

(65) Chaumont, A.; Wipff, G. *Inorg. Chem.* **2004**, *43*, 5891.

(66) Dai, S.; Shin, Y. S.; Toth, L. M.; Barnes, C. E. *Inorg. Chem.* **1997**, *36*, 4900.

(67) Chaumont, A.; Wipff, G. *Phys. Chem. Chem. Phys.* **2005**, *7*, 1926.

Upon dissolution of uranyl triflate, perchlorate, and nitrate salts in Tf_2N -based ILs, the anions likely remain, at least partially, coordinated to uranyl, according to spectroscopy results. In the case of the nitrate salt, the two nitrates remain, on the average, coordinated to uranyl, leading to a mixture of complexes including $\text{UO}_2(\text{NO}_3)_3^-$.

Although no experimental data could be obtained for the UO_2X_2 salts in the C_4mimPF_6 solution, MD results predict that the nitrate, perchlorate, and sulfate anions should also remain coordinated. In the case of nitrates, the higher preference for this state, compared to the dissociated salt, is more pronounced in C_4mimPF_6 than in $\text{C}_4\text{mimTf}_2\text{N}$, in keeping with the weaker coordination properties of PF_6^- compared to Tf_2N^- . Thus, although ionic liquids are inherently ionic in nature and polar, they seem to be less dissociating than water, where the nitrates are dissociated at the studied concentrations.

Conclusion

To summarize, as in the case of Eu(III) ,³⁰ the solubility and coordination properties of uranium(VI) in room-temperature ionic liquids markedly depend on the chemical form under which uranium(VI) is introduced in solution, on the composition of the IL, and on the presence of any additional anions. The interplay of the different anionic species as potential uranyl ligands should also strongly influence the complexation properties toward neutral or negatively charged molecules (e.g., TBP, CMPO, calixarenes with acidic binding functionalities). It can also be surmised that small amounts of impurities (e.g., cocrystallized water with the uranyl salt) also contribute to the thermodynamic and kinetic features of the dissolution of the salt in the ionic liquid and to its reactivity.

Acknowledgment. This work was supported by ACTINET and the GDR PARIS. A.C. and G.W. are grateful to IDRIS, CINES, Université Louis Pasteur, and PARIS for computer resources and to Etienne Engler for assistance. A.C. thanks the Alexander von Humboldt Foundation for a fellowship.

Supporting Information Available: Summary of the solubility of uranyl salts in studied ILs, characteristics of the simulated systems, complexation energies (in kcal/mol) of uranyl complexes in the gas phase calculated by molecular mechanics (MM) and by QM methods, MM charges, atomic charges used for the MM and MD simulations, fit of the shoulder on the Fourier transform at $R + \Delta \sim 1.80 \text{ \AA}$. This material is available free of charge via the Internet at <http://pubs.acs.org>.

IC061864+